Glow-Discharge Flow Visualization in Low-Density Free Jets

S. S. FISHER* AND D. BHARATHAN†
University of Virginia, Charlottesville, Va.

Glow discharges have been formed in low-density supersonic free jets for purposes of flow visualization. The free jets are formed by expansion through an orifice at high pressure ratio. Discharges are generated using d.c., 60-Hz a.c., rf, and impulsive (tesla-coil) excitation. Electrode arrangements are such that the imposed fields are well defined. The gases N_2, air, CO_2, He, Ar, H_2, and O_2 have been employed as the discharge medium, with the obtained flow-visualization quality decreasing roughly in the order listed. Flows with and without a spherical model submerged in the jet have been examined. The rf excitation yields superior flow visualization at higher relative density levels; tesla-coil excitation yields better flow visualization at lower relative densities; dc excitation is inferior at all density levels. Combinations of excitation are superior for visualizing flows about models.

I. Introduction

THE formation of a glow discharge in a flowing gas as a means for visualizing flow features has been employed for a number of years. In the present study, a systematic set of experiments using some standard and some not-so-standard means for exciting the discharge has been performed. The purpose of these experiments has been to explore and to better define the characteristics and utility of the technique.

The term "glow discharge" as employed here refers to the luminous, weakly ionized plasma that can be caused to occur in relatively low density gases in the presence of a suitable electric field. Glow discharges in quiescent gases, easily produced in most gases at pressures typically from 10^{-2} to 10 torr, have been studied extensively and are well understood. [1-3] In flowing gases, since molecular speeds are negligible compared to electron speeds and since excited states of molecules (except for metastable species) are of negligible duration compared to most important molecular transit times, the glow-discharge mechanisms are essentially identical to those in a quiescent gas. Even so, in fast flowing gases, where fluid density gradients can be quite large, the discharge can differ substantially in appearance. Moreover, the existence of metastable species can lead to the appearance of "afterglow," i.e., relaxation of species well downstream of the point of excitation.

The relationship between the distribution of fluid density and the observed distribution of luminosity depends upon the type of excitation, the type of electrodes, the gas, etc. Regardless of this complexity, in a discharge where a shock wave is present, the density jump across this wave generally gives rise to a change in luminosity. Also, in regions where the fluid density gradient is high compared to the gradient in the electric field, the luminosity generally increases with increasing density. Appreciation of these two characteristics of glow discharges in flowing gases will be sufficient for the present study.

Glow-discharge flow visualization (shortened to GDFV, hereafter) is useful only to the extent that the flow is not substantially affected by the discharge. Typically, the power input to the discharge is a few watts per liter and the mole fractions of ions and excited species are each less than 10^{-4}. Thus, it is expected and easily confirmed (see later on) that the discharge has little effect on the fluid motion.

Received March 2, 1972; revision received June 11, 1973.
Research supported by AFOSR Grant 69-1798.
Index categories: Rarefied Flows; Jets, Wakes, and Viscid-Inviscid Flow Interactions.

* Associate Professor of Aerospace Engineering.
† Graduate Student. Student Member AIAA.

Of course, glow discharge formation is only one of several means for visualizing low-density flows. The electron-beam fluorescence method[4,5] is applicable over a broader range of gas density and from it one can obtain quantitative density and energy-state information. The afterglow method,[6-8] particularly useful with nitrogen, has been used for flow visualization at higher density levels. Techniques for specific gases based on excitation of molecules by photons, X-rays, etc., also exist.[5,9] Even so, since the glow-discharge method requires little special instrumentation, it can often be employed to advantage.

Several published accounts of successfully developed GDFV methods exist. Kane[8] used 60-Hz, 2500-v a.c. (and higher) excitation of high speed air and N_2 flowing through an acrylic nozzle. Enkenhus[10] visualized flows exiting from a nozzle by connecting a repeat-firing, automobile-type ignition coil to a metal ring surrounding the flow. Bomelburg[11] visualized flow in a standard supersonic wind tunnel by applying to a centrally located model a positive potential of several thousand volts relative to grounded tunnel walls. Potter et al.[12] achieved visualization of a uniform hypersonic N_2 flow by connecting a tesla coil to a model submerged in the flow. Kalugin[13] reports flow visualization with a d.c. discharge in uniform, low-density, hypersonic N_2 flows exiting from a nozzle; the nozzle was the cathode and the anode was far to one side of the flow. McCroskey et al.[14] employed an 800-v d.c. discharge between a laterally located cathode and wind-tunnel walls to visualize hypersonic, low-density N_2 flow near a flat plate. Horstman and Kussoy[15] visualized hypersonic, low-density He and air flows by impressing −300-v d.c. (relative to tunnel walls) on conical models in the flows. Cassanova and Wu[16] briefly describe the use of rf excitation to visualize the interaction between opposed supersonic jets. Horstman[17] describes use of a d.c. glow discharge in large, hypersonic, low-density freejets of air and He by placing −300-v d.c. (presumably relative to either the jet orifice or chamber walls) on a model in the flow. Finally, Coudeville et al.[18] report visualization of uniform, hypersonic, low-density N_2 flows by striking a d.c. discharge between a cylindrical model (submerged in crossflow) and auxiliary cylindrical electrodes located symmetrically to either side of the flow.

Most experimenters have favored the d.c. mode of GDFV. Only Kalugin,[13] however, gives a reasonably complete account of his technique. Among those using other than the d.c. mode, only Kane[8] and Enkenhus[10] give substantial technical details.

II. Experimental Details

The present investigation was carried out in a small, hypersonic, free jet-type wind tunnel. A diagram of the tunnel is shown in Fig. 1. The flow exhausts from an acrylic

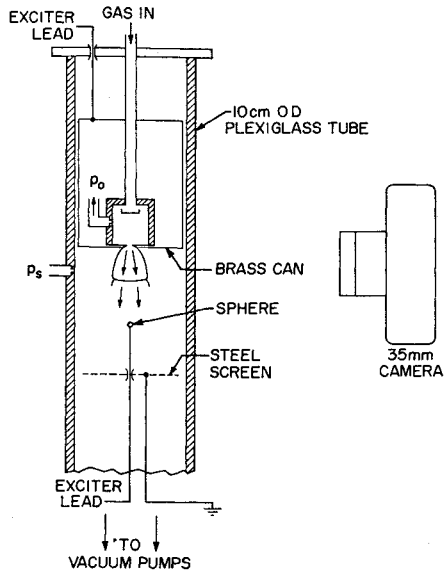

Fig. 1 Diagram of the apparatus.

stagnation chamber through a 2.5-mm-diam, sharp-edged brass orifice into a 9-cm inside-diameter acrylic tube. The gas is then conducted through a blower-type vacuum pump (0.6 m^3/sec) to a standard-type vacuum pump (0.2 m^3/sec) which exhausts it to the atmosphere. Operation is continuous. Electrodes to establish the exciting field include 1) a thin brass can (with top open) surrounding the stagnation chamber, 2) a grounded, 1-cm-mesh steel screen nominally 10 cm downstream of the can's lower surface, and, if present, 3) a 3-mm-diam steel ball (a bearing ball) spot-welded to a thin stainless steel sting. The bottom surface of the can, positioned about 1 mm below the jet orifice, is provided with a 1-cm-diam hole which allows the jet to pass through unhindered. The brass can and grounded screen are not essential. The jet-orifice plate itself could be used as one electrode and grounded parts downstream in the wind tunnel could serve as a second electrode. The functions of the can were to eliminate local edge glows that appeared when the orifice plate was employed as an electrode, to minimize sputtering of the orifice plate, and to provide a more uniform exciting field for the free jet. The grounded screen better defined the imposed excitation field; its precise position, so long as it was downstream of the shock waves which make up the free jet Mach bottle[19] (also see Fig. 1), had little effect on GDFV of that Mach bottle.

Photographs of the discharge in the vicinity of the Mach bottle have been obtained with a 35-mm camera using fine-grained film (Kodak Pan-X, ASA 32) and an f-stop of 4.0. Exposure times are quoted in the figures. To minimize light reflection, the can's lower surface was covered with lampblack and the inner wall of the wind tunnel opposite the camera was covered with flat black paper.

To excite the discharges, a regulated d.c. power supply (0–1000 v, 0–200 ma), a laboratory-type tesla coil, and a radio-frequency (rf) power supply (27 MHz, nominally 800 v peak to peak and 100 w maximum output) were used. The tesla coil, when allowed to discharge into quiescent air, exhibited a strongly damped sinusoidal potential with peak amplitude about 20,000 v, with period 2.4 μsec, and with half-amplitude decay time about 1 period. This pulse repeated itself approximately 100 times/sec. When exciting a nitrogen discharge, the peak amplitude typically dropped to about 1500 v but the other quoted characteristics did not change.

For d.c. discharges, the can was made the cathode, i.e., it was biased negatively with respect to the grounded screen. (For the opposite arrangement, viz., biasing the can positively with respect to the grounded screen, it was difficult to sustain a discharge and flow visualization was much poorer.) For rf and tesla-coil discharges, the respective power sources were connected directly to the can. Most rf and some d.c. discharges were self starting. However, for most d.c. discharges and many rf discharges, starting was most readily accomplished by placing the tesla coil momentarily near the can.

All gases employed were of standard commercial purity. Stagnation pressure p_0 was monitored with a capacitance manometer and a Hg U-tube manometer. Wind-tunnel static pressure p_s was measured with McLeod a gauge. Gas stagnation temperature was nominally 300 K for all flows.

III. Results

Of all the gases tested, nitrogen exhibited the best glow discharge flow visualization, regardless of the type of excitation (GDFV for air was virtually identical to that for nitrogen). Typical examples of GDFV in nitrogen jets are shown in nine photographs in Fig. 2 where, for each of the three types of excitation, the resulting glow pattern at three different stagnation pressures is exhibited.

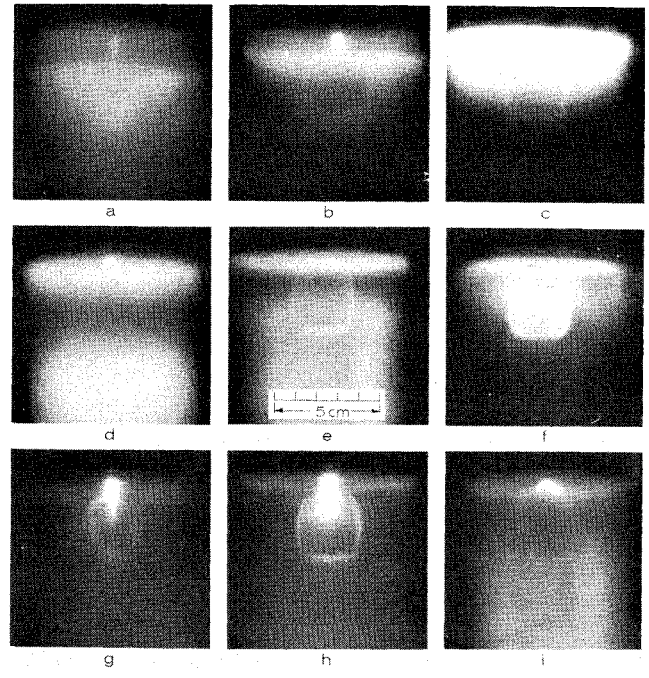

Photo-graph	Can excitation	p_0(torr)	p_s(torr)	Dominant color	Exposure time (s)
a	d.c. (−700)[a]	30	0.80	violet	2.0
b	d.c. (−700)	120	0.22	violet	0.1
c	d.c. (−500)	240	0.46	violet	0.1
d	rf (15)[b]	30	0.08	rust-red	0.1
e	rf (15)	120	0.22	rust-red	0.02
f	rf (45)	620	1.10	rust-red	0.1
g	tesla	30	0.08	reddish-pink	0.1
h	tesla	120	0.22	violet	0.1
i	tesla	620	1.10	violet	0.1

[a] For d.c. excitation, the number in parentheses is the applied cathode potential relative to ground (v).

[b] For rf excitation, the number in parenthesesis approximately the output power of the rf supply (w).

Fig. 2 GDFV for N_2 jets at differing density levels using three different modes of excitation.

GDFV obtained with d.c excitation (Figs. 2a–2c) was faint and/or low in contrast. Glow features arising from shock waves tended to be masked by the glow appearing in the approximately stagnant background gas surrounding the jet. With increasing pressure, the d.c. discharge increased in brightness up to $p_0 \approx 250$ torr and then decreased rapidly in both brightness and extent with further increase in p_0. Brightness also increased with increasing electric field. To first approximation, however, contrast was independent of brightness. For d.c. fields greater than those employed for these photographs, electrical breakdown occurred intermittently near the orifice. At higher p_0, this breakdown occurred at lower fields. It was later discovered that higher fields could be imposed if a suitable electrical resistance was placed in series with the power supply. However, no such resistance was employed when the photographs here were taken.

Flow visualization obtained with rf excitation (Figs. 2d–2f) was much better than that obtained with d.c. excitation, particularly at higher pressures. Glow brightness increased up to $p_0 \approx 500$ torr and then decreased, but GDFV was effective up to 1000 torr. Brightness also increased with rf power level (see figure captions; the power levels for these photographs were the maximum the power supply could transmit to each given discharge). Again, contrast was not first-order dependent on brightness. While at intermediate pressures (Fig. 2e) the shock waves themselves were brightest, at higher p_0 (Fig. 2f) the lower density region upstream of the shock glowed more brightly. This behavior at higher pressure is thought to be due to quenching of the glow at the density levels existing downstream of these shock waves.

With tesla-coil excitation (Figs. 2g–2i), while free jet shock structure was better resolved at low p_0 than with d.c. or rf excitation, at high p_0 flow definition was inferior to that obtained with rf, primarily because of lack of brightness. This decreased brightness is believed to result from the limited power capacity of the tesla coil. With tesla-coil excitation, the bright core near the orifice always appeared. This core, blue in color and often ragged in shape, resembled a corona-type breakdown and presumably resulted from the combined presence of stronger electric fields and higher gas densities near the orifice.

In all photographs in Fig. 2, the glow in the background gas surrounding the jet exhibits its own distinct features. For d.c. excitation, these features include the usual cathode (upper) and negative (lower) glows observed in quiescent discharges. Somewhat surprisingly, for rf and tesla-coil excitation, similar features are seen. Since the outputs of the rf power supply and the tesla coil were not referenced to ground (they sought their own mean d.c. level), these features are thought to result, at least in part, from the buildup of a negative d.c. potential on the cathode as a result of the imposed excitation. Experiments where the cathode was purposefully biased while being rf or tesla-coil driven support this hypothesis.

While the upper limit on gas density where GDFV is effective depends on such things as available power and, for d.c. excitation, circuit stability, the lower density limit does not. For d.c. excitation, this lower limit was defined by a density level below which the discharge could not be sustained. For rf and tesla-coil excitation, as p_0 was decreased below approximately 30 torr, the discharge gradually shrank toward the orifice and, below $p_0 = 20$ torr, it crept into the region upstream of the orifice. At these low values of p_0, Mach bottle visualization was also complicated by concomitant thickening of shock waves.

In Fig. 2, note that the Mach bottle size and shape remain unchanged with change in excitation mode (all photographs in this figure are to the same scale). Size and shape were also found to be invariant with change in exciter power level. Moreover, the measured axial positions of the Mach disk (that almost normal shock which forms the base of the Mach bottle) relative to the jet orifice agree well with those determined by other means elsewhere.[19] These observations offer convincing proof that the discharges do not affect these flows to appreciable extent.

Table 1 Results of GDFV investigations with gases other than N

Gas	Effective modes of excitation	Effective p_0-range (torr)	Dominant color	GDFV quality	Brightness relative to N_2
CO_2	rf, tesla, d.c.	10–1000	Deep blue	Good	Slightly less
He	tesla, rf	10–1000	Pale green and/or pink	Fair	Slightly less
Ar	rf, tesla	10–300	Violet	Fair	Much less
H_2	tesla	10–200	Bluish white	Fair	Much less
O_2	rf	Above 500	Greenish yellow	Poor	Very faint

GDFV with the gases He, H_2, O_2, Ar, and CO_2 was also investigated rather thoroughly as part of this study. The modes of excitation effective for GDFV, the range of p_0 over which GDFV was achieved, discharge colors, and GDFV quality relative to N_2 are listed in Table 1. In less extensive tests, methane, acetylene, and acetone also were employed. Notwithstanding a few exceptions, these investigations indicate that gases with more complex molecular structure are better candidates for GDFV.

Combined modes of excitation can lead to improved flow visualization, particularly when a model is submerged in the flow. As an indication of this improvement, GDFV attained with a number of different mode combinations is illustrated in Fig. 3. For the photographs in this figure, the flow geometry and scale are the same as in Fig. 2 except for the fact that the previously described sphere has been positioned on the jet axis 2 cm downstream of the jet orifice. For this figure the gas is N_2 and $p_0 = 120$ torr.

For initial reference, Fig. 3a shows the flow for tesla-coil excitation applied to the can with the model ungrounded. Here, the sphere's bow shock wave is easily resolved all the way to its intersection with the free jet barrel shock (that shock which forms the side of the Mach bottle). A second shock wave originating just behind the sphere was faintly evident to the eye but is not easily resolved in the photograph. This second wave was surely present, however, since its intersection with the bow wave is the only logical explanation for the observed kink in that wave. There is no indication in the photograph of a Mach disk downstream of the sphere, but since the observed bow-shock shape requires supersonic flow to exist downstream of its outer portions, this Mach disk still must have been present in some form.

To illustrate the benefit of combining modes, Fig. 3b shows the same case as in Fig. 3a except with the model now rf excited in addition. This auxiliary excitation is seen to bring out the shock waves more clearly, but unfortunately, it also is seen to produce a bright sheath around the model and sting. Tests conducted in stagnant gases show that this sheath bears no relationship to the flow. If, instead of auxiliary rf excitation, a potential of up to ± 400-v d.c. was imposed on the model, there resulted no change from the GDFV exhibited in Fig. 3a.

As a second reference case, Fig. 3c shows the discharge observed with rf instead of tesla-coil excitation applied to the can, again with the model ungrounded. Here the model/sting sheath is also observed (not as bright as in Fig. 3b) and shock-wave resolution is poorer than in Fig. 3b due to the brighter glow in the background gas. When tesla-coil excitation was added to the model, there was no change from that shown in Fig. 3c. However, when a positive potential of several hundred volts was impressed on the model, the shock layer ahead of the sphere glowed more brightly. For the model at 200-v d.c., this brighter glow is exhibited in Fig. 3d.

As a third reference, Fig. 3e shows a d.c. discharge in the jet, here too with the model floating. For this excitation,

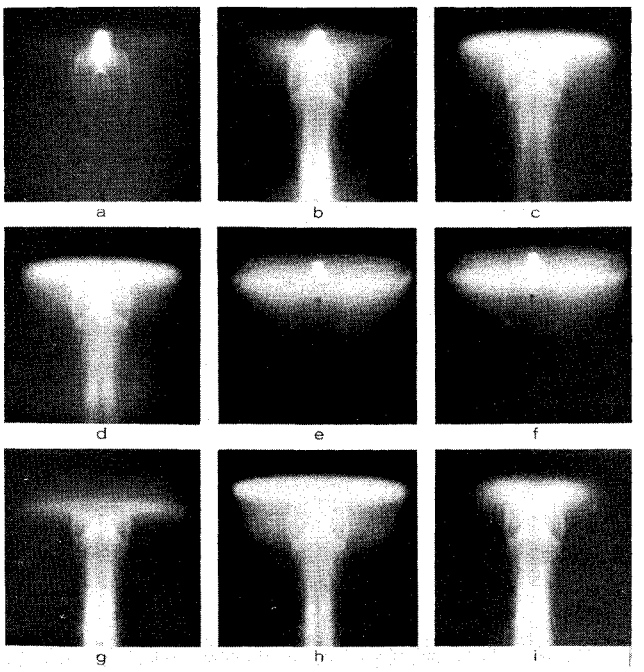

Photograph	Can excitation	Model excitation	Remarks
a	tesla	floating	good FV except for corona near orifice.
b	tesla	rf (50)	same as (a), except for model/sting rf sheath.
c	rf (35)	floating	good FV except for bright layer near can.
d	rf (35)	d.c. (+200)	same as (c), except for narrow model/sting sheath.
e	d.c. (−700)	floating	marginal FV.
f	d.c. (−600)[a]	tesla	same as (e) except bow shock more evident.
g	d.c. (−450)[a]	rf (50)	upper-region FV poorer, lower-region FV better than (e).
h	floating	rf (50)	similar to (c).
i	d.c. (+200)	rf (50)	background glow suppressed compared to (h).

[a] Because of cross coupling of exciters, −700-v d.c. could not be maintained for these photographs.

Fig. 3 GDFV for N_2 flow about 3-mm-diam sphere positioned on free jet axis 2 cm from jet orifice using various combinations of can/model excitation; $p_0 = 120$ torr, $p_s = 0.22$ torr, film exposure time = 0.1 sec.

the sphere's bow shock and the free jet barrel shock are only faintly evident. The shock layer ahead of the sphere could be brightened by adding tesla-coil excitation to the model (Fig. 3f) but the brightness of other shock waves was not increased. Addition of rf instead of tesla-coil excitation to the model (Fig. 3g) brought out all the shock waves more clearly (except next to the can, where the discharge was suppressed altogether) and suggested that rf model excitation was a mode to be pursued further.

The best combination of excitation found for this particular flow and electrode arrangement was that of rf model excitation combined with a positive d.c. potential on the can. Excitation of the model alone, as illustrated in Fig. 3h, brought out the various shock waves rather clearly but also produced a bright background glow. Fortunately, this glow could be suppressed by applying nominally 200-v d.c. to the can. The resulting GDFV, the best achieved, is shown in Fig. 3i.

For conditions other than those in this figure, this "best" combination of modes was found to provide reasonable delineation of shock waves over a range of p_0 from 10 to 1000 torr for all positions of the model within the Mach bottle except those within a few millimeters of the can. Within the stated p_0 range, the glow was generally brighter and shock waves were more distinct at higher p_0. At low p_0, masking due to background glow was a problem.

As a supplementary part of this investigation, a 60-Hz a.c. potential was applied to the can. For this, the amplitude V_a and mean d.c. level V_m were adjustable. Satisfactory GDFV for this excitation was obtained when $V_m - V_a$ was several hundred or more volts negative. When this was so, the discharge was similar in appearance to that obtained with a d.c. potential equal to $V_m - V_a$ applied to the can. To first approximation, the ratio V_a/V_m was not important in determining the nature of the discharge.

In these tests, the rf and tesla-coil discharges were not confined to the region near the electrodes. Strong tail glows sometimes stretched as far as a meter down the exhaust manifold. It is difficult to estimate what parts of these tail glows were due to the exciting field being transmitted downstream and what parts were due to relaxation of metastables (afterglow). The shapes of these tails were such that they followed the expected streaming motion of the gas rather closely. In several tests where the flow was again accelerated to slightly supersonic speed in a downstream section of the manifold (accomplished by introducing a suitable choke), various shock waves in the manifold could be easily resolved in the tail glow.

In characterizing the flows in this investigation, the stagnation pressure p_0 has been employed. In the figures, the static pressure outside the jet has also been quoted. These two pressures together with an appreciation for the gas dynamics of free jets[19] are sufficient to characterize the density distribution in the regions photographed. For given electrical excitation, it is this density distribution as a whole, of course, which determines the character of the discharge.

IV. Conclusions

The wind tunnel in this study, with its small size and substantial lack of metal parts, was well suited to the excitation approaches employed here. Even so, the basic techniques in this investigation should find application in many other sorts of low-to-medium density, high-speed flows. Of the devices employed, the tesla coil is the simplest and, at lower density levels, the best for GDFV. To be effective at higher density levels, a tesla coil with higher output power than the one employed here (~ 10 w) probably is needed. The superiority of rf excitation at higher gas densities is evident in the present results. However, this may well result from the higher output power (~ 100 w) of the rf exciter employed, With both tesla-coil and rf excitation, a serious disadvantage is electrical interference with other electronic instruments. When such interference must be avoided, the d.c. discharge, even though it provides poorer GDFV, will have to be employed.

With regard to the combining of excitation modes to obtain improved flow visualization, the results depicted here should be considered illustrative. In other situations with differing electrode and flow geometries, other combinations may yield better results. The point to be made is that joining of modes can lead to superior GDFV and the investigator should anticipate the possible benefit of such combination.

References

[1] Cobine, J. D., *Gaseous Conductors*, Dover, New York, 1958.
[2] Llewellyn-Jones, F., *Ionization and Breakdown in Gases*, Methuen, London, 1957.
[3] Brown, S. C., *Basic Data of Plasma Physics*, MIT Press, Cambridge, Mass., 1959.

[4] Maguire, B. L., Muntz, E. P., and Mallin, J. R., "Visualization Technique for Low-Density Flow Fields," *IEEE Transactions*, Vol. AES-3, No. 2, March 1967, pp. 321–326.

[5] Sherman, F. S. and Hurlbut, F. C., *Rarefied Gas Dynamics*, National Committee on Fluid Dynamics Films, Encyclopedia Brittanica, 1970.

[6] Williams, T. W. and Benson, J. M., "Preliminary Investigation of the Use of Afterglow for Visualizing Low Density Compressible Flows," TN 1900, June 1949, NACA; also see Benson, J. M., "Measurements of the Physical Properties of Active Nitrogen," *Journal of Applied Physics*, Vol. 23, No. 7, July 1952, pp. 757–763.

[7] Kunkel, W. B. and Hurlbut, F. C., "Luminescent Gas Flow Visualization for Low Density Wind Tunnels," *Journal of Applied Physics*, Vol. 28, No. 8, Aug. 1957, pp. 827–835.

[8] Winkler, E. M., "Electrical Discharge and Afterglow Technique," *Physical Measurements in Gas Dynamics and Combustion*, Vol. IX, *High Speed Aerodynamics and Jet Propulsion*, Princeton Univ. Press, Princeton, N.J., 1954, pp. 79–88.

[9] Winkler, E. M., "Spectral Absorption Method," and "X-Ray Technique," *Physical Measurements in Gas Dynamics and Combustion*, Vol. IX, *High Speed Aerodynamics and Jet Propulsion*, Princeton Univ. Press, Princeton, N.J., 1954, pp. 89–96 and 97–108.

[10] Enkenhus, K. R., "The Design, Instrumentation, and Operation of the UTIA Low-Density Wind Tunnel," Rept. 44, June 1957, Univ. of Toronto Inst. of Aerospace Studies, Toronto, Ontario, Canada.

[11] Bomelburg, H. J., "A New Glow-Discharge Method for Flow Visualization in Supersonic Wind Tunnels," *Journal of the Aerospace Sciences*, Vol. 25, No. 11, Nov. 1958, pp. 727–728.

[12] Potter, J. L., Kinslow, M., Arney, G. D., Jr., and Bailey, A. B., "Initial Results from a Low Density Hypervelocity Wind Tunnel," *Hypersonic Flow Research*, Vol. 7, Academic Press, New York, 1962, pp. 599–624.

[13] Kalugin, V. M., "Ultrasensitive Glow Discharge Method for Visualizing Hypersonic Flows of Rarefied Gases," *Journal of Applied Mechanics and Technical Physics*, Vol. 7, No. 4, July–Aug. 1966, pp. 75–78.

[14] McCroskey, W. J., Bogdonoff, S. M., and McDougall, J. G., "An Experimental Model for the Sharp Flat Plate in Rarefied Hypersonic Flow," *AIAA Journal*, Vol. 4, No. 9, Sept. 1966, pp. 1580–1587.

[15] Horstman, C. C. and Kussoy, M. I., "Hypersonic Viscous Interaction on Slender Cones," *AIAA Journal*, Vol. 6, No. 12, Dec. 1968, pp. 2364–2371.

[16] Cassanova, R. A. and Wu, Y-C. L., "Flow Field of a Sonic Jet Exhausting Counter to a Low-Density Supersonic Airstream," *Physics of Fluids*, Vol. 12, No. 12, Dec. 1969, pp. 2511–2514.

[17] Horstman, C. C., "Surface Pressures and Shock-Wave Shapes on Sharp Plates and Wedges in Low-Density Hypersonic Flow," *Rarefied Gas Dynamics*, Supplement 5, Vol. 1, Academic Press, New York, 1969, pp. 593–605.

[18] Coudeville, H., Viviand, H., Raffin, M., and Brun, E. A., "An Experimental Study of Wakes of Cylinders at Mach 20 in Rarefied Gas Flows," *Rarefied Gas Dynamics*, Supplement 5, Vol. 1, Academic Press, New York, 1969, pp. 881–894.

[19] Ashkenas, H. and Sherman, F. S., "The Structure and Utilization of Supersonic Free Jets in Low Density Wind Tunnels," *Rarefied Gas Dynamics*, Supplement 3, Vol. 2, Academic Press, New York, 1966, pp. 84–105.